Chalcogenide Letters Vol. 16, No. 5, May 2019, p. 209 - 214

NANOSECOND PULSED LASER GENERATION WITH BISMUTH (III) TELLURITE SATURABLE ABSORBER

R. Z. R. R. ROSDIN[a], A. A. A. JAFRY[b], S. W. HARUN[a], N. F. ZULKIPLI[a], Z. JUSOH[c], M. YASIN[d*]

[a]*Photonics Engineering Laboratory, Department of Electrical Engineering, University of Malaya, 50603 Kuala Lumpur, Malaysia*

[b]*Department of Physics, Faculty of Science, Universiti Teknologi Malaysia, 81310 Skudai, Johor, Malaysia.*

[c]*Faculty of Electrical Engineering, Universiti Teknologi Mara (Terengganu), 23000 Dungun, Terengganu, Malaysia*

[d]*Department of Physics, Faculty of Science and Technology, Airlangga University, Surabaya (60115) Indonesia*

We demonstrated nanosecond pulsed fiber laser operating at 1563 nm by using a newly developed Bismuth (III) Telluride (Bi_2Te_3) based saturable absorber (SA). The SA was obtained by embedding Bi_2Te_3 material into polyvinyl Alcohol (PVA) film. By incorporating the SA into a 209 m long cavity Erbium-doped fiber laser (EDFL), a stable nanosecond pulses were generated. It operated at repetition rate of 1.8 MHz with a pulse width of 193 ns and a signal-to-noise ratio (SNR) of 58 dB. The newly developed Bi_2Te_3 SA has a potential to be further enhanced towards better generation of ultrashort pulse fiber lasers.

(Received March 4, 2019; Accepted May 9, 2019)

Keywords: Bismuth (III) Telluride, Passive saturable absorber, Bi_2Te_3, Nanosecond pulses

1. Introduction

Nanosecond pulsed lasers have obtained significant interests in recent years because of their potential applications in many science and technology fields. Their unique properties in terms of temporal and spectral characteristics make them become important in many fields such as multi-photon microscopy, industrial materials processing, biomedical imaging, microwave generation, remote sensing and all-fiber optics telecommunication technologies [1-3]. To date, many techniques have been used to generate nanosecond pulses including the nonlinear Kerr lensing, intensity/phase modulation, and saturable absorption. Among these techniques, saturable absorption of the material was the simplest and thus passively mode-locked Erbium-doped fiber lasers (EDFLs) have been intensively investigated. Unlike the active method that employed an electrical signal-driven modulator inside the laser cavity, the passive mode-locking approaches does not require any external signal for pulse creation. Thus, they are preferable since they are more compact in geometry, simpler and producing a higher efficiency. The generation of pulses can be passively realized through the insertion of saturable absorber (SA) into the laser cavity and this arrangement gives more advantages to their output pulses characteristics [4-5].

Semiconductor saturable absorber mirrors (SESAMs) were widely employed as SA in commercial laser systems. Generally, the absorbers use hetero-structure quantum wells, which was deposited onto a distributed Bragg grating (DBG) through molecular beam epitaxy (MBE) or metal-organic chemical vapor phase deposition (MOCVD) processes [6]. Therefore, they inherent many drawbacks including complex fabrication process and complex packaging procedure. They also have a relatively narrow operation bandwidth due to narrow bandwidth of DBGs and the limited energy bandgap of semiconductors. To overcome this problem, various low-dimensional

*Corresponding author: yasin@fst.unair.ac.id

nanomaterials have been demonstrated as SA since they have remarkable optical properties such as ultrafast carrier dynamics and high third-order nonlinear susceptibility [7-9]. These materials include carbon nanotubes (CNTs) and graphene. For CNTs, the absorption wavelength is determined by the nanotube diameter, and thus they are not really efficient. Graphene was attractive as demonstrated in many laser experiments. But it has a low modulation depth of less than 2 % per layer [9].

Besides graphene, other two-dimensional (2D) materials have also gained interests for both electronic and photonics applications. These materials include black phosphorus (BPs), transition metal dichalcogenides (TMDs) and topological insulator (TIs), which have been reported to possess unique optical properties such as Pauli blocking induced saturable absorption [10-13]. Among these materials, TIs have attracted more research interest due to their large modulation depth property, which can make saturable absorption becomes more efficient [10-11]. Previously, Q-switched fiber lasers were demonstrated using Bismuth (III) Selenide (Bi_2Se_3) SAs [14-15]. In this paper, we used a Bismuth (III) Tellurite (Bi_2Te_3), which was embedded into polyvinyl Alcohol (PVA) film as a passive SA to generate nanosecond pulses in the EDFL cavity. By incorporating the film inside a long laser cavity, a stable nanosecond mode-locked fiber laser was generated to operate at 1563 nm region with repetition rate of 1.8 MHz.

2. Preparation and optical characterization of SAs

In this work, we develop a new film-based SA with Bi_2Te_3 as the absorber material to integrate into an EDFL cavity for nanosecond pulses generation. We used the commercially available few-layer Bi_2Te_3 powder (Sigma Aldrich) with molecular weight 800.76 g/mol. The host polymer was prepared by dissolving 1 g of polyvinyl Alcohol (PVA) (Sigma Aldrich) in 120 ml de-ionized (DI) water. The mixture was stirred at room temperature using a magnetic stirrer. To prepare a SA film, 14 mg of Bi_2Te_3 was mixed with 3 ml of the prepared PVA solution. The mixture was thoroughly mixed with the aid of a magnetic stirrer for three hours. The Bi_2Te_3-PVA solution was then placed in ultrasonic bath for 10 minutes to fully bind the powder with the PVA. After that, the Bi_2Te_3 suspension was obtained and it was carefully poured onto petri dish. It was then left to dry at room temperature for 2 days to form Bi_2Te_3-PVA composite film.

The developed film was characterised using a Field-Emission Scanning Electron Microscope (FESEM) as shown in Fig. 1(a). As seen in the figure, the Bi_2Te_3 film has a high density of micro-rods and micro-grains, which were distributed randomly on the substrate surface. These micro-rods and micro-grains are in irregular shapes and their average diameters are in a range of 0.5-1.9 μm. To confirm their optical saturable absorption property, the nonlinear optical response for the Bi_2Te_3 film was also investigated based on dual optical power meter techniques. The pulse input source used was a mode-locked fiber laser, which has femtosecond output pulse with a 17 MHz repetition rate and a 900fs pulse duration, which the output power is approximately 5 mW. The obtained transmission curve is shown in Fig. 1(b). It indicates the modulation depth of 30%, non-saturable absorption of 55% and saturation intensity of approximately 40 MW/cm^2. Fig. 1(c) shows the image of the fabricated film, which was placed onto a fiber ferrule. The absorption curve of the film is illustrated in Fig. 1 (d), which indicates the absorption loss of about 3.5 dB at 1550 nm region.

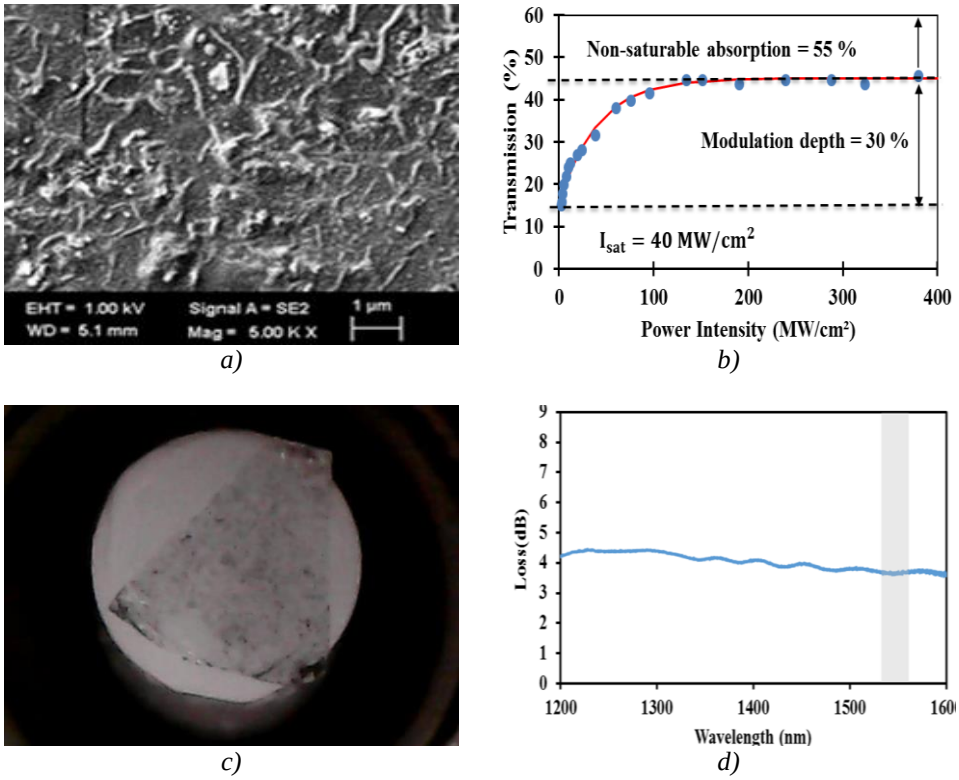

Fig. 1. Bi_2Te_3 characteristics (a) FESEM image (b)nonlinear absorption curve (c) image of the SA film onto the fiber ferrule (d) Absorption loss spectrum.

3. Experimental setup

The schematic diagram of the proposed nanosecond pulses EDFL is illustrated in Fig. 2. It based on all-fiber ring cavity using the newly developed Bi_2Te_3 PVA film as a SA. A 2.8 m long Erbium-doped fiber (EDF) was used as the gain medium. It has a high absorption coefficient of 23 dB/m at 980 nm with a core diameter of 4 µm and a numerical aperture of 0.16. The EDF was forward pumped by a 980 nm pump laser through a 980/1550 nm wavelength division multiplexer (WDM). A polarization independent isolator was incorporated into the EDFL cavity to prevent the bidirectional transmission in the laser cavity. The SA device was constructed by sandwiching a tiny piece of the prepared Bi_2Te_3 PVA film between two fiber ferrules via a fiber adapter to form a fiber-compatible device. Index matching gel was applied at the fiber connection to minimize parasitic reflections. The insertion loss of the SA device was recorded as about 2 dB at 1560 nm. In the proposed laser cavity, we added a 198 m long SMF to tailor the dispersion and nonlinearity characteristics inside the cavity so that nanosecond pulses can be generated. An 80/20 coupler was used to monitor output laser emission. An Optical Spectrum Analyzer (OSA: Yokogawa, AQ6370B) and an oscilloscope (GWINSTEK: GDS-3352) with high speed photodetector were used to monitor the spectral characteristics and the pulse trains, respectively. 7.8 GHz Radio Frequency (RF) spectrum analyzer (Anritsu MS2683A) was used to monitor the repetition rate and stability of the mode-locked laser. The average output power was measured by the power meter (ILX Lightwave OMM-6810B) coupled with its power head (ILX Lightwave OMH-6727B InGaAs). The laser cavity has a total length of approximately 109 m.

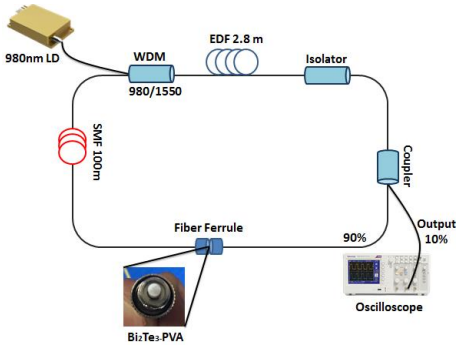

Fig. 2. Configuration of the nanosecond mode-locked EDFL with Bi_2Te_3 PVA film as a SA.

4. Results and discussion

The performance of the EDFL based on Bi_2Te_3 PVA film SA was investigated by varying the power of the 980 nm pump. The continuous wave (CW) laser was firstly obtained as the power hit the threshold of 44 mW. Then, a self-starting and stable pulses train was obtained when the pump power reached the mode-locking threshold of 96 mW. This threshold power is relatively high due to the long lased cavity and high insertion loss of the SA film. The mode-locking operation was also observed to maintain stable as the pump power was further increased up to 121 mW. Fig. 3(a) shows the oscilloscope trace of the mode-locked pulse train at the threshold pump power. The time interval between the pulses is about 0.548 μs, that matches with cavity length of 109 m. The pulse period is equivalent to repetition rate of 1.8 MHz. The pulse width of laser was kept at around 193 ns, when adjusting the value of pump power from 96 to 121 mW.

Fig. 3 (b) compares the output spectrum of the EDFL with and without the SA when the 980 nm pump power was fixed at 96 mW. Without the SA, the laser operated in at 1569 nm due to the employment of a relatively long EDF. The continuous wave (CW) laser operation was based on the energy transfer from a short wavelength of around 1525 nm to a longer wavelength above 1560 nm in a quasi-two-level laser system. As shown in Fig. 3(b), the laser operating wavelength shifted to a shorter wavelength of 1563 nm with the incorporation of SA inside laser cavity, which change the laser operation from CW to mode-locking regime. This is attributed to the cavity loss, which increased with the incorporation of SA. The operating wavelength shifted to a shorter wavelength region which has a higher gain to compensate for the loss.

The stability of the laser was also investigated by measuring the radio frequency (RF) output spectrum as illustrated Fig. 3(c). We only observed the fundamental and the harmonic frequencies in the RF output spectrum, which further confirmed the stability of the mode-locking operation. The fundamental frequency was obtained at 1.83 MHz, which is in good agreement with the oscilloscope trace. The RF spectrum shows the fundamental frequency has a signal to noise ratio of 58 dB, which indicates that the generated laser pulsing is very stable.

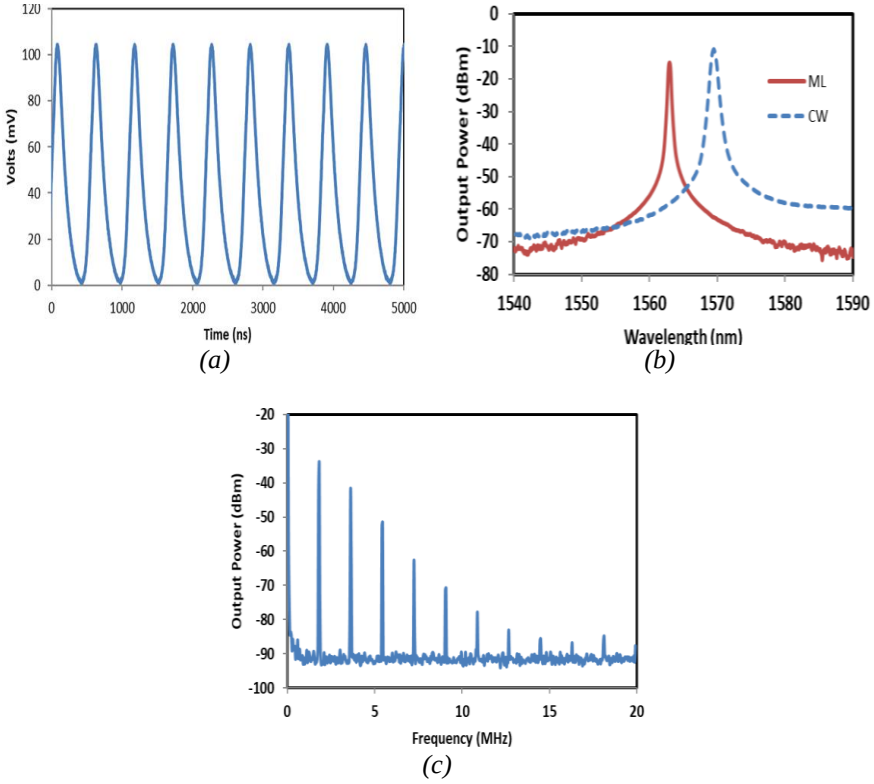

Fig. 3. Mode-locking performances (a) typical pulse train (b) output spectrum with and without the SA (c) RF spectrum.

Fig. 4 shows the measured average output power and single pulse energy against the pump power. As seen in the figure, the threshold pump power of 96 mW produces the lowest output power of 2.65 mW. At 121 mW pump power level, the output power was 3.49 mW. The output power increased linearly as the 980nm pump power increased, significantly give the optical-to-optical efficiency of 3.4 %. Each of single pulse train consists relatively 1.92 nJ pulse energy at 121 mW pump power. It is worthy to note that the pulses train was unstable above 121 mW pump level where the pulsing generation was suppressed with further increase of the pump power, and no pulse train observe in oscilloscope. The mode-locking performance could be further improved by optimizing the fabrication method of the Bi_2Te_3 thin film, reducing the cavity loss and increasing the strength of the interaction between the SA and the laser pulses.

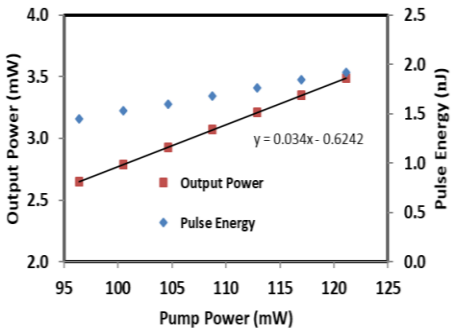

Fig. 4. Average output power and single pulse energy against pump power.

5. Conclusions

The nanosecond mode-locked laser was successfully demonstrated using the prepared Bi_2Te_3 PVA film as SA. Self-starting and stable mode-locked pulses train was obtained to operate at 1565 nm region as the SA was incorporated into a 209 m long EDFL cavity. The mode-locked laser operated at repetition rate of 1.8 MHz with a pulse width of 193 ns and a SNR of 58 dB.

Acknowledgements

This work is financially supported by Airlangga University - Mandate Research Grant (2019) and the University of Malaya (GPF005A-2019).

References

[1] R. Woodward, R. Howe, G. Hu, F. Torrisi, M. Zhang, T. Hasan, E. J. R. Kelleher, Photonics Research **3**, A30 (2015).
[2] S. Yefet, A. Peer, Applied Sciences **3**, 694 (2013).
[3] F. Quinlan, T. M. Fortier, M. S. Kirchner, J. A. Taylor, M. J. Thorpe, N. Lemke, A. D. Ludlow, Y. Jiang, S. A. Diddams, Optics Lett. **36**, 3260 (2011).
[4] A. Nady, M. Baharom, A. Latiff, S. Harun, Chinese Phys. Lett. **35**, 044204 (2018)
[5] Y. M. Chang, J. Lee, J. H. Lee, Japanese Journal of Applied Phys. **51**, 072701 (2012).
[6] U. Keller, K. J. Weingarten, F. X. Kartner, D. Kopf, B. Braun, I. D. Jung, R. Fluck, C. Honninger, N. Matuschek, J. Aus der Au, IEEE Journal of selected topics in Quantum Electronics **2**, 435 (1996).
[7] M. Mahyuddin, A. Latiff, M. Rusdi, N. Irawati, S. Harun, Opt. Commun. **397**, 147 (2017).
[8] N. Kasim, A. H. H. Al-Masoodi, F. Ahmad, Y. Munajat, H. Ahmad, S. W. Harun, Chinese Optics Letters **12**, 031403 (2014)
[9] Q. Bao, H. Zhang, Y. Wang, Z. Ni, Y. Yan, Z. X. Shen, K. P. Loh, D. Y. Tang, Advanced Functional Materials **19**, 3077 (2009).
[10] H. Haris, H. Arof, A. R. Muhammad, C. L. Anyi, S. J. Tan, N. Kasim, S. W. Harun, Optical Fiber Technology **48**, 117 (2019).
[11] A. H. H. Al-Masoodi, F. Ahmad, M. H. M. Ahmed, H. Arof, S. W. Harun, Optical Engineering **56**(5), 056103 (2017).
[12] A. A. Latiff, M. F. M. Rusdi, Z. Jusoh, M. Yasin, H. Ahmad, S. W. Harun, Optoelectron. Adv. Mat. **10**, 801 (2016).
[13] M. B. Hisyam, M. F. M. Rusdi, A. A. Latiff, S. W. Harun, IEEE Journal of Selected Topics in Quantum Electronics **23**, 39 (2017).
[14] H. Ahmad, M. R. K. Soltanian, L. Narimani, I. S. Amiri, A. Khodaei, S. W. Harun, IEEE Photonics Journal **7**(3), 1 (2015).
[15] H. Haris, S. W. Harun, A. R. Muhammad, C. L. Anyi, S. J. Tan, F. Ahmad, R. M. Nor, N. R. Zulkepely, H. Arof, Optics & Laser Technology **88**, 121 (2017).